

[Reprinted from THE AERONAUTICAL JOURNAL OF THE ROYAL AERONAUTICAL SOCIETY, November 1985]

# **Notes on the structure of viscous and numerically-captured shocks**

**J. PIKE\***

# Notes on the structure of viscous and numerically-captured shocks

J. PIKE\*

## SUMMARY

An exact expression for the flow variables through a viscous shock wave is obtained from the Navier-Stokes equations. The Prandtl number is taken to be  $3/4$ , which is close to the value for air, and the viscosity is assumed to be given by Sutherland's formula.

By considering the limit as the viscosity tends to zero, it is shown that the solution to the Euler equations has an entropy spike at the shock wave. This explains certain, hitherto considered spurious, features of shock waves captured by numerical solutions of the Euler equations.

## 1. INTRODUCTION

Analytic solutions of the Navier-Stokes equations are of interest, both for the insight they can give into the nature of the solution flow and as possible test examples to validate computer programs designed to compute more general flows. One of the few analytic solutions available for the viscous compressible Navier-Stokes equations is the steady flow through a plane shock wave, which has been derived using a simplified form of the viscosity-temperature relationship<sup>(1,2)</sup>. A more accurate analytic solution, using Sutherland's formula for the viscosity, is presented here. Although the new solution produces results largely similar to those obtained previously, it is nevertheless important because it removes the uncertainty introduced by using less accurate viscosity temperature relationships.

There has been much discussion<sup>(3-7)</sup> on the validity of these solutions when applied to strong shock waves in air, because the shocks may be so thin that air ceases to behave as a continuous medium in equilibrium. It would appear both from limitations imposed by the assumption of thermal equilibrium<sup>(5)</sup>, as well as direct comparison of the solutions of the Navier-Stokes equations with solutions of the Boltzmann equation<sup>(6,7)</sup>, that the Navier-Stokes profiles are valid up to a maximum normal Mach number of about 1.5. Within this Mach number restriction however, because most shock waves are very nearly plane on a scale related to shock wave thickness, the profiles have wide application to shock waves in air.

Most variables vary smoothly and monotonically through the shock wave from their upstream to their downstream value. The entropy, however, has a maximum within the shock wave<sup>(3)</sup>. In Section 5 an expression for the height of this maximum is derived, which does not depend on the viscosity-temperature relationship. As the viscosity tends to zero, the Navier-Stokes equations reduce to the Euler equations and the shock wave becomes a discontinuity without internal structure.

\*The research reported in this paper was carried out while the author was at RAE, Bedford.  
Paper No 1311.

However, the maximum value of the entropy at the shock wave remains finite. Thus the solution of the Euler equations, when considered as a limiting case of the Navier-Stokes equations, has an entropy spike at the shock wave. This provides some justification for the 'spurious' entropy spikes which occur in some numerical solutions of the Euler equations.

## 2. NOTATION

$A_1 - A_4$	constants defined after equation (12)
$b$	constant in Sutherland's formula (equation (5))
$c$	constant defined in equation (8)
$c_p, c_v$	specific heat at constant pressure and volume
$d$	constant defined in equation (9)
$I_1 - I_4$	functions of $u, \gamma, M_1$ and $b$ defined in equations (13-16)
$k_1 - k_4$	constants defined after equation (12)
$M_1$	Mach number far upstream and normal to the shock wave
$p$	pressure
$R$	gas constant ( $c_p - c_v$ )
$T$	absolute temperature
$u$	velocity normal to the shock wave (later non-dimensionalised by $u_1$ )
$x$	co-ordinate in direction normal to shock wave
$x_R$	reference length $\mu_1/\rho_1 u_1$
$\gamma$	ratio of specific heats
$\mu$	coefficient of viscosity
$\rho$	density

## Subscripts

1	far upstream
2	far downstream
$x$	differentiation in direction normal to shock wave

## 3. REDUCED NAVIER-STOKES EQUATIONS

The flow is assumed to be steady with constant conditions far upstream and far downstream, where the pressure, density, temperature and velocity components in the  $x$  and  $y$  directions are given by  $p_1, \rho_1, T_1, u_1, v_1$  and  $p_2, \rho_2, T_2, u_2$  and  $v_2$  respectively. The specific heats at constant pressure,  $c_p$ , and volume,  $c_v$ , are assumed to be constant and the equation of state is to be taken to be that of a perfect gas.

ie

$$p = \rho RT \quad \dots \quad (1)$$

where  $R$  is the gas constant,  $c_p - c_v$ .

We seek solutions to the reduced Navier-Stokes equations, when there is no change in the flow variables in the  $y$ -direction

and the transverse velocity  $v$  is constant everywhere. With these assumptions and a value of Prandtl number of 3/4, which is close to the value for air, the mass, energy and momentum equations reduce to<sup>(5,8)</sup>

$$\rho u = \rho_1 u_1 \quad \dots (2)$$

$$u^2 + 2c_p T = (\gamma + 1) u_1 u_2 / (\gamma - 1) \quad \dots (3)$$

$$\rho_1 u_1 (u_1 - u) (u - u_2) = -\frac{8\gamma}{3(\gamma + 1)} \mu u u_x \quad \dots (4)$$

where  $\mu$  is the coefficient of viscosity,  $\gamma$  is the ratio of specific heats,  $c_p/c_v$ , and  $u_x = du/dx$ .

The only term remaining to be defined is the coefficient of viscosity in equation (4), and this is most adequately described by Sutherland's formula<sup>(5)</sup>,

$$\mu \propto T^{3/2} / (T + T_0)$$

where  $T_0$  is often taken to be 114K. For our purposes we use the form of the formula suggested by Pia<sup>(8)</sup>, that is

$$\frac{\mu}{\mu_1} = \frac{(T/T_1)^{3/2} (1 + b)}{(T/T_1) + b} \quad \dots (5)$$

where  $b$  is a constant inversely proportional to  $T_1$  and the suffix 1 denotes a reference condition, here taken to be on the upstream side of the shock. Because of the complication of Sutherland's formula a more algebraically convenient form of  $\mu$  is sometimes used, namely

$$\mu = \text{constant } T^\omega \quad \dots (6)$$

where  $\omega$  is a constant whose value for air is usually taken to be<sup>(5,8)</sup> between 3/4 and 1. The available solutions of Becker<sup>(1)</sup> Thomas<sup>(2)</sup> and Howarth<sup>(5)</sup> use equation (6) with  $\omega = 0$  and 1/2 respectively. While noting that a further analytical solution using equation (6) with  $\omega = 1$  could be obtained, we proceed instead to derive the more accurate analytical profiles using Sutherland's formula. It is shown later that the errors for the  $\omega = 1$  solution must be expected to be similar in magnitude to those for  $\omega = 1/2$ .

#### 4. ANALYTIC SOLUTION

Substitution for the temperature in Sutherland's formula from equation (3) gives

$$\frac{\mu}{\mu_1} = \frac{(1 + b) (c^2 - u^2)^{3/2}}{(c^2 - 1)^{1/2} (d^2 - u^2)} \quad \dots (7)$$

where  $u$  is non-dimensionalised with respect to  $u_1$ , and the constants  $c$  and  $d$  are expressed in terms of the upstream Mach number normal to the shock wave ( $M_1$ ) by

$$c^2 = \frac{(\gamma + 1)u_2}{(\gamma - 1)} = 1 + \frac{2}{(\gamma - 1)M_1^2} > 1 \quad \dots (8)$$

and

$$d^2 = c^2 + (c^2 - 1)b = 1 + \frac{2(1 + b)}{(\gamma - 1)M_1^2} > c^2 \quad \dots (9)$$

Substituting for  $\mu$  in equation (4) from equation (7) we can write  $u_x$  as a function of  $u$

ie

$$\frac{\mu u_x}{\rho_1} = \frac{-3(\gamma + 1) (c^2 - 1)^{1/2} (1 - u) (u - u_2) (d^2 - u^2)}{8\gamma (1 + b) u (c^2 - u^2)^{3/2}} \quad \dots (10)$$

This equation can be integrated to give

$$-\frac{3(\gamma + 1) (c^2 - 1)^{1/2} x}{8\gamma (1 + b) x_R} = \int \frac{(c^2 - u^2)^{3/2} u du}{(1 - u) (u - u_2) (d^2 - u^2)} \quad \dots (11)$$

where  $x_R$  is the reference length  $\mu_1/\rho_1 u_1$ . It can be observed that  $x/x_R$  has the form of a Reynolds number in the upstream flow normal to the shock wave.

By using the substitution  $u = c \sin \theta$ , the RHS can be written

$$I = \sum_1^4 \frac{c^3}{A_i} \int \frac{\cos^4 \theta d\theta}{k_i + \sin \theta} \quad \dots (12)$$

where  $A_1$  to  $A_4$  have values  $2(d - 1)(d - u_2)$ ,  $2(d + 1)(d + u_2)$ ,  $-(d^2 - 1)(1 - u_2)$  and  $(d^2 - u_2)(1 - u_2)/u_2$  respectively, and  $k_i$  has values  $-d/c$ ,  $d/c$ ,  $-1/c$  and  $-u_2/c$ . The four integrals which are summed in equation (12) have been evaluated to give

$$I_1 = 2(d^2 - c^2)^{3/2} \tan^{-1} \left\{ \frac{c^2 + c(c^2 - u^2)^{1/2} + du}{(c + (c^2 - u^2)^{1/2})(d^2 - c^2)^{1/2}} \right\} + q_1 \quad \dots (13)$$

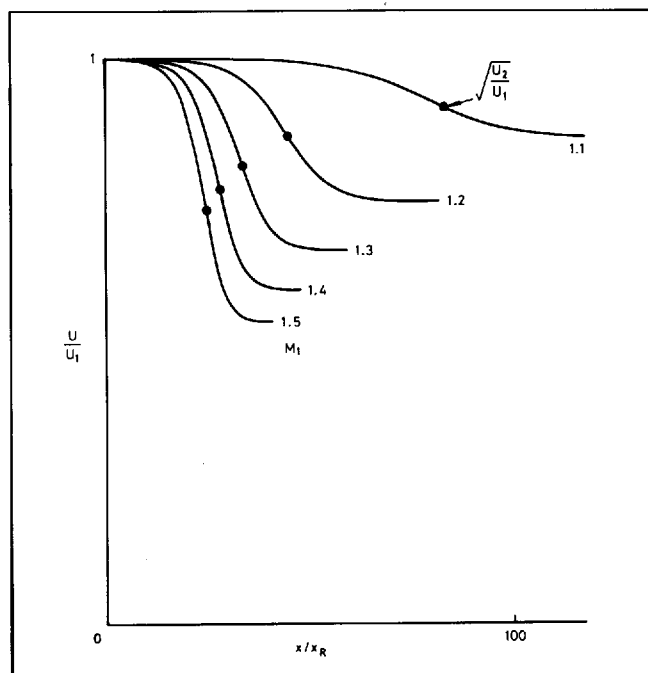


Figure 1. Shock wave profiles for various upstream Mach numbers with  $\gamma = 1.4$  and  $b = 0.522$ .

$$I_2 = 2(d^2 - c^2)^{3/2} \tan^{-1} \left\{ \frac{c^2 + c(c^2 - u^2)^{1/2} + du}{(c + (c^2 - u^2)^{1/2})(d^2 - c^2)^{1/2}} \right\} + q_2 \quad \dots (14)$$

$$I_3 = -2(c^2 - 1)^{3/2} \coth^{-1} \left\{ \frac{c^2 + c(c^2 - u^2)^{1/2} - u}{(c + (c^2 - u^2)^{1/2})(c^2 - 1)^{1/2}} \right\} + q_3 \quad \dots (15)$$

$$I_4 = -2(c^2 - u_2^2)^{3/2} \tanh^{-1} \left\{ \frac{c^2 + c(c^2 - u^2)^{1/2} - u_2 u}{(c + (c^2 - u^2)^{1/2})(c^2 - u_2^2)^{1/2}} \right\} + q_4 \quad \dots (16)$$

where  $q_i$  is given by

$$q_i = c^3 k_i \left( \frac{3}{2} - k_i^2 \right) \sin^{-1} (u/c) + \frac{1}{6} (c^2 - u^2)^{1/2} (8c^2 - 6c^2 k_i^2 + 3ck_i u - 2u^2) \quad \dots (17)$$

With  $I_1$  to  $I_4$  given by equations (13) to (16),  $x/x_R$  is expressed as an analytic function of  $u$ ,  $M_1$ ,  $\gamma$  and  $b$  by

$$\frac{x}{x_R} = - \frac{8\gamma(1+b)}{3(\gamma+1)(c^2-1)^{1/2}} \left\{ \frac{I_1}{A_1} + \frac{I_2}{A_2} + \frac{I_3}{A_3} + \frac{I_4}{A_4} \right\} \quad \dots (18)$$

The other flow variables can be expressed in terms of  $u$  using equations (1) to (3).

Shock wave profiles from equation (18) with  $\gamma = 1.4$  are shown in Fig. 1 plotted against  $x/x_R$ . The value of  $b$  used is that suggested by Pia<sup>(8)</sup>, namely  $b = 0.522$  when  $T_1 = 222K$ . The origin of the  $x/x_R$  axis is chosen for clarity to be upstream of the shock wave. The  $x$  position for critical conditions, where  $u = (u_1 u_2)^{1/2}$ , is shown on each profile. The most striking feature of the profiles is the rapid decrease in shock wave width with increasing Mach number. In Fig. 2, profiles for  $M = 1.5$  with  $b = 0.522$  (continuous curve) and  $b = 0$  (dotted curve) are shown. We see that as  $b$  increases from 0 to 0.522 the shock wave width increases by about 5%. When  $b = 0$  Sutherland's formula reduces to the form of expression used for  $\mu$  by Thomas<sup>(2)</sup>.

More generally, the error in the shock wave width incurred by using equation (6) can be estimated from the error in  $u_x$  within the shock wave. At critical conditions within the shock wave when  $u = (u_1 u_2)^{1/2}$  we have from equations (3) and (8)

$$\frac{T_{crit}}{T_1} = \frac{1 + (\gamma - 1)M_1^2}{\gamma + 1}$$

and from equation (4) for any value of  $u$

$$\begin{aligned} \frac{u_x \text{ (approximate)}}{u_x \text{ (Sutherland)}} &= \frac{\mu \text{ (Sutherland)}}{\mu \text{ (from equation (6))}} \\ &= \frac{(T/T_1)^{3/2-\omega}(1-b)}{(T/T_1) + b} \end{aligned}$$

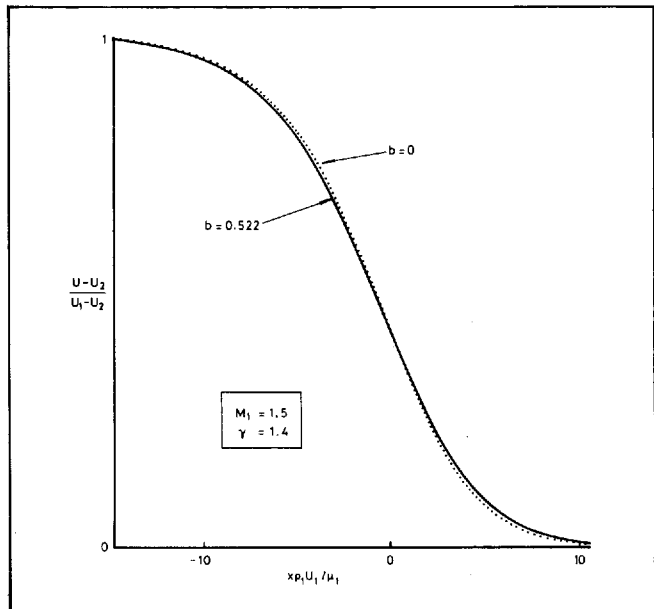


Figure 2. Shock wave profiles from Sutherland's formula with  $b = 0$  and  $0.522$ .

Then using the same values for  $T_1$  and  $b$  as above, the shock width error must be expected to increase nearly linearly with Mach number, from zero at sonic conditions to  $-12\%$ ,  $-6\%$  and  $5\%$  when  $\omega = 0$ ,  $1/2$  and  $1$  respectively at  $M_1 = 1.5$ .

## 5. ENTROPY SPIKES AND SHOCK CAPTURING ALGORITHMS

As  $\mu \rightarrow 0$ , equations (2)-(4) reduce to the one-dimensional Euler equations and the shock wave width tends to zero. At the shock wave the variables have values which jump discontinuously from the upstream conditions (1) to the downstream conditions (2). This discontinuous change in the flow variables causes problems for numerical computation of the flow using shock capturing algorithms, in that spurious oscillations tend to be produced in the numerical solution near the discontinuity. To control this oscillatory behaviour, terms similar to the  $\mu u_x$  term in equation (4) have long been added to the equations<sup>(9)</sup> to introduce a large numerical viscosity near the shock wave. The internal structure of these numerical shock waves depends on the type of term added.

It has been assumed in the past that successful shock wave representation should produce monotonic changes from upstream to downstream conditions by means of a few intermediate values<sup>(10)</sup>. However, some algorithms cause peak values to occur at the shock wave<sup>(11)</sup>, particularly in variables such as the entropy, and these 'spurious' features have been regarded as resulting from the oscillatory tendency of the algorithm near the shock wave. In Fig. 3 we show the analytic distribution of  $p/\rho^\gamma$  through the shock wave as a function of  $x/x_R$ . We see that this variable has a maximum within the shock wave and that in the limit as  $\mu \rightarrow 0$ , the distribution becomes a spike. The entropy is directly expressible in terms of this variable

$$S - S_1 = c_v \ln \left\{ \frac{p/\rho^\gamma}{p_1/\rho_1^\gamma} \right\} \quad \dots (19)$$

and hence the entropy will also peak at the shock wave<sup>(3)</sup> and have a spike as its limit. From equations (1)-(3) this maximum value is found as a function of  $M_1$  and  $\gamma$  to be

$$S_{\max} = S_1 + c_v \ln \left\{ M_1^2 \left( \frac{\gamma - 1}{\gamma + 1} + \frac{2}{(\gamma + 1)M_1^2} \right)^{\frac{\gamma+1}{2}} \right\} \quad (20)$$

at a velocity of  $(u_1 u_2)^{1/2}$ . The values of  $(S_{\max} - S_1)$  as a ratio to the rise in the entropy through the shock wave  $(S_2 - S_1)$ , are plotted in Fig. 4 for  $\gamma = 1.4$ . At  $M = 1.5$ , we see that the entropy peaks at a value of over twice the rise through the shock wave. At smaller Mach numbers the relative rise is greater, but the entropy rise across the shock wave is much smaller, as is indicated by the plots in Fig. 3.

As the maximum entropy given by equation (20) is derived without using equation (4), it is independent of the viscosity. Thus the approximate solutions based on the viscosity assumptions of equation (6) with  $\omega = 0, 1/2$  and  $1$ , will exhibit the correct entropy maximum within the shock wave. As  $\mu \rightarrow 0$  for any of the solutions, the entropy distribution will become a spike at the shock wave.

For the case of zero viscosity, equations (2)-(4) can be identified as the Euler equations of mass, energy and momentum respectively. Thus, any scheme for obtaining steady solutions of the Euler equations which conserves mass and energy and obeys the equation of state, will be correct in exhibiting an entropy maximum at the shock wave as prescribed by equation (20).

## CONCLUSIONS

An exact solution for the flow through a viscous shock wave is found by solving the Navier-Stokes equations with a Prandtl number of  $3/4$  and Sutherland's Law for the viscosity-temperature relationship. The values of the flow variables through the shock wave are found to differ by only a small amount from values found previously using less accurate viscosity-temperature relationships. The main difference is an increase in the width of the shock wave by about 5%.

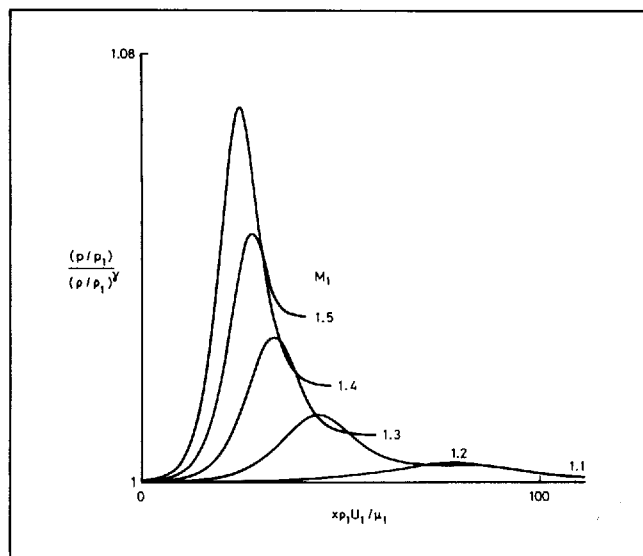


Figure 3. Variation of  $p/p_1$  through the shock wave, with  $b = 0.522$ .

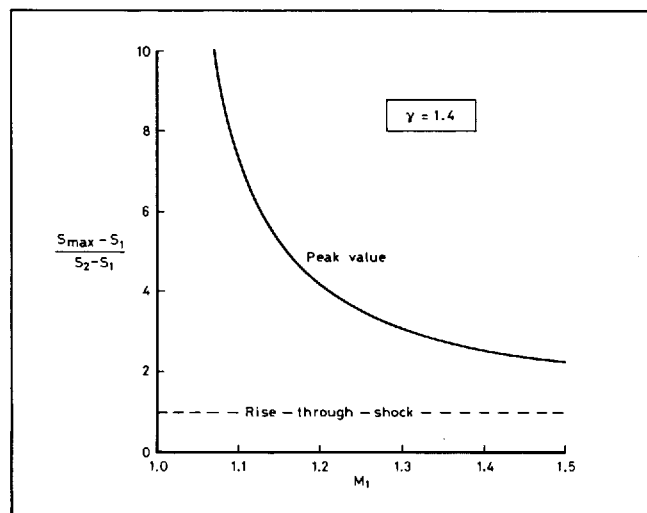


Figure 4. Ratio of entropy peak to entropy rise through the shock wave.

This solution, like previous solutions, shows that the entropy has a local maximum within the shock wave. The height of this maximum is found as a function of the normal Mach number upstream of the shock wave, and it is independent of the viscosity. Thus, if we regard the Euler equations as a reduced form of the Navier-Stokes equations as the viscosity tends to zero, the solution to the Euler equations has an entropy spike at the shock wave. More particularly, solutions of the steady Euler equations which conserve mass and energy and obey the equation of state have as their solution an entropy spike of zero thickness at the shock wave, whose height is related to the normal upstream Mach number. The occurrence of this entropy spike provides an explanation for the 'spurious' entropy spikes which occur in some numerical solutions of the Euler equations.

## REFERENCES

1. BECKER, R. Stobewelle und Detonation. *Z. Phys*, 1921, **8**, 321.
2. THOMAS, L. H. Note on Becker's theory of the Shock Front. *J Chem Phys*, 1944, **12**, 449-53.
3. MORDUCHOW, M. and LIBBY, P. A. On a complete solution of the one-dimensional flow equations of a viscous, heat-conducting, compressible gas. *J Aero Soc*, 1949, **16**, 11, 674.
4. GILBARG, D. and PAOLUCCI, D. The structure of shock waves in the continuum theory of fluids. *J of Rational Mech Anal*, 1953, **2**, 617.
5. HOWARTH, L. Modern developments in fluid dynamics, high speed flow. Oxford University Press, 1953, **1**.
6. LIEPMANN, H. W., NARISIMA, R. and CHAHINE, M. T. Structure of a plane shock layer. *Phy of Fluids*, November 1962, **5**, 11, 1313-24.
7. HICKS, B. L., YEN, S. M. and REILLY, B. J. The internal structure of shock waves. *J Fluid Mech*, 1972, **53**, 1, 85-111.
8. PIA, S. Viscous flow theory, 1 Laminar flow, D. Van Nostrand Co Inc, 1956.
9. VON NEUMANN, J. and RICHTMYER, R. D. A method for the numerical calculation of hydrodynamic shocks. *J of Applied Phy*, March 1950, **21**, 3, 232-237.
10. ROE, P. L. An introduction to numerical methods suitable for the Euler equations. VKI Lecture Series Note, An introduction to computational fluid dynamics, 1983-01.
11. RIZZI, A. and VIVIANI, H. Numerical methods for the computation of inviscid transonic flows with shock waves. Proceedings of the GAMM Workshop, Stockholm 1979. Vieweg 1981.